COMBINED BIOMATERIALS: AMNIOTIC MEMBRANE AND ADIPOSE TISSUE TO RESTORE INJURED BONE AS PROMOTER OF CALCIFICATION IN REGENERATION. PRECLINICAL MODEL.

Katherine Carvalho[1], Dilcele Silva Moreira Dziedzic[1], Júlio César Francisco[1], Bassam Felipe Mogharbel[1], Ana Carolina Irioda[1], Priscila Elias Ferreira Stricker [1], Paulo André Bispo Machado Júnior[1], Juliana Floriano[1], Lúcia de Noronha[1], Luiz Cesar Guarita-Souza[1], Eltyeb Abdelwahid[1], and Célia Regina Cavichiolo Franco[1]

[1]Affiliation not available

July 31, 2020

Posted on Authorea 31 Jul 2020 — CC0 1.0 — https://doi.org/10.22541/au.159620994.43378706 — This a preprint and has not been peer reviewed. Data may be preliminary.

INTRODUCTION

Bone presents continuous remodeling and a generous regenerative capacity compared to other tissues. Life-long bone remodeling is responsible for skeletal development, responses to mechanical stimuli, and maintaining mineral homeostasis. Intrinsic regeneration capacity guarantees bone integrity as an injury repair process. Moderate-sized bone defects repair without the need for a graft. However, complex clinical conditions are requiring a considerable amount of bone, in which natural bone regeneration capacity is not sufficient to establish functional tissue recovery. In the case of significant bone defects created by trauma, infection, skeletal disorders, or in the treatment of tumor excision, the regeneration process becomes compromised [1].

Strategies may be necessary to guide or accelerate the process, increasing bone quantity or quality [2]. There is intense research in bone bioengineering, seeking to overcome the limitations observed in non-healing defects and alternative methods to autologous bone grafts, in order to produce bone substitutes with the same properties of this gold standard [3]. Osteoconduction is the process of perivascular tissue, precursor, and osteoprogenitor cell ingrowth, from the bony bed into implanted frameworks. Osteoinduction is the induction of undifferentiated mesenchymal stem cells into osteoprogenitor cells, also at ectopic sites [4]. The combination of three-dimensional biocompatible frameworks with cells and growth factors may stimulate osteogenesis and osteoinduction, enhance the osteogenic capacity of transplanted and endogenous cells and thus, ensure better healing [5].

Calvarial "non-healing" defects are useful in the preclinical study of bone repair to analyze strategies of tissue engineering in intramembranous bone formation. Some advantages of this defect are the orthotopic non-load bearing site, its reproducibility, mechanical stability, and the limited baseline healing plateau, above which the effect of cell/scaffold implant on osteogenesis is noticeable [6-9]. The application of membranes is indicated for Guided Bone Regeneration (GBR), to isolate the bone defect from other tissues, and for bone reconstruction [10]. Commercially available collagen membranes are widely used in *in vivo* studies, associated with ceramic implant material [11], demineralized bone matrix [3], growth factors [12], and cells [13]. The membranes covering bone defects in calvaria provided stability for ceramic tricalcium phosphate (TCP) inserted into the defect, resulting in higher bone amount and better mechanical properties [11]. The association of ceramic and membrane with bone marrow mesenchymal stem cells have been demonstrated to favor earlier bone deposition [13]. Calvarial "non-healing" defects are effective in the preclinical study of

bone repair to analyze strategies of tissue engineering in intramembranous bone formation. Some advantages of this defect is the orthotopic non-load bearing site, its reproducibility, mechanical stability, and the limited baseline healing plateau, above which the effect of cell/scaffold implant on osteogenesis is noticeable [6-10].

Commercially available collagen membranes are widely used in *in vivo* studies, associated with ceramic implant material [11], demineralized bone matrix [3], growth factors [12] and cells [13]. The membranes covering bone defects in calvaria provided stability for TCP inserted into the defect, resulting in higher bone amount and better mechanical properties [11]. The association of ceramic and membrane with bone marrow mesenchymal stem cells has been demonstrated to favor earlier bone deposition [13].

Tissues that are mainly available in maternity hospitals, and often discarded, can be a reliable source of allogenous cells and collagenous matrix for bone tissue engineering applications. Importantly, umbilical cord mesenchymal stem cells have been shown to stimulate vascularization and bone formation *in vivo* [14, 15]. In addition, amniotic membranes are known to be a source of stem cells and collagenous scaffold [16, 17]. Mesenchymal stem cells from amniotic membranes can stimulate osteogenic and angiogenic differentiation of various cell sources, including, adipose-derived stem cells [18]. Moreover, amniotic membranes present great potential in clinical application [19], tissue engineering [17], and the removal of the epithelial cell layer minimizes the risks of adverse immunological responses [20, 21].

Amniotic membrane association with stem cells from bone marrow [22] and adipose tissue [23, 24] demonstrated that Decellularized Human Amniotic Membrane (DAM) is an excellent cell-carrier in tissue regeneration applications. Bone and periodontal tissue engineering studies have demonstrated that DAM can provide a preferential environment for osteogenic differentiation of dental apical papilla cells, increase the expression of osteogenic marker genes, and deposition of mineralized matrix *in vitro* [25]. Periodontal ligament stem cells transfer onto DAM [26], and ASCs cultured on DAM [27] have been shown to stimulate periodontal regeneration *in vivo* . Interestingly, double-layered cell transfer technique on DAM allowed transplantation of periodontal ligaments stem cells and osteoblasts, and enhanced bone formation in calvaria when compared to single-cell type transplantation [28]. The application of amniotic membrane in calvarial defects has been found to promote more significant bone regeneration compared to defect without graft, but less than the association with ceramic material (HA) and osteoinductive factor Bone morphogenetic protein (BMP) [29]. Interestingly, DAM associated with ASCs were also used successfully in a calvarial defect in rabbits [24].

Studies using multipotent ASCs, since their first reports [30, 31] have demonstrated their potential as a significant source of adult stem cells in regenerative medicine. Some significant advantages of ASCs in bone engineering compared to Bone Marrow Stem Cells are the facility in harvesting, higher cellular yield, and proliferation capacity [32]. The application of the patient autologous cells from fat, transferred in order to enrich and accelerate the bone regeneration process was reported, in cranioplasties associated with TCP [33], in maxillary defect associated with titanium, TCP, BMP [34], and graft [35].

Earlier studies investigating calvarial defects without cell expansion from the adipose tissue have used various materials, including fragmented adipose tissue [36, 37], Stromal Vascular Fraction (SVF) associated with polylactide (PLA), demineralized bone matrix (DBM) [38], and hypertrophic cartilage [39]. After isolation, ASCs were investigated as perivascular cells associated with poly(lactic-co-glycolic acid) (PLGA)/ hydroxyapatite (HA) composites [9, 40], stem cells associated with PLGA [41], stem cells associated with PLGA/HA composites [40, 42-48], stem cells associated with Whitlockite [49], with acellular collagen dermal matrix [50], with HA/TCP bioceramics and hydrogel [51], silicate bioceramic [52], and duck-beak bioceramic [53].

Investigations on ASCs participation in calvarial bone defect repair have reported the occurrence of significant cell migration to the lesion site after intravenous cell administration [42], and paracrine effect of ASCs on *in vitro* and *in vivo* osteoblastic cell differentiation [47]. There was a significantly higher stimulation in cell association of immediately prepared defects, compared to cell graft with established bone defects [46]. There is considerable evidence indicating that ASCs cells may contribute to periodontal regeneration [54]. Our results demonstrated enhanced *in vivo*bone regeneration by undifferentiated adipose-derived stromal cells loaded onto a decellularized human amniotic membrane.

Posted on Authorea 31 Jul 2020 — CC0 1.0 — https://doi.org/10.22541/au.159620994.43378706 — This a preprint and has not been peer reviewed. Data may be preliminary.

MATERIALS and METHODS

The experimental design consisted primarily of the decellularization of a human amniotic membrane, expansion of adipose tissue-derived stromal cells from rats, and preparation of scaffolds for the treatment of non-healing calvarial defects of rats. The human placenta was collected in accordance with The Code of Ethics of the World Medical Association [55], only after approval of the Research Ethics Committee of Complexo Hospitalar Pequeno Príncipe and co-participating institution (Curitiba, Brazil; Number 659.204, 09/03/2015). The informed consent form obtained from a mother undergoing natural childbirth at the Hospital Maternidade Victor Ferreira do Amaral (Curitiba, Brazil), after clinical screening for diseases. All experiments with animals complied with the ARRIVE guidelines [56], the national guidelines for the care and use of laboratory animals, and followed the protocols approved by the Animal Care Ethics Committee of Faculdades Pequeno Príncipe (Curitiba, Brazil; Number 039-2018, 22/11/2018).

The amniotic membrane was collected immediately after placental expulsion in the surgical environment. With blunt dissection, the amniotic membrane was separated from the chorion and kept in Phosphate buffer saline (PBS 2% streptomycin/penicillin). The fresh membrane, handled within a laminar flow Class II Biosafe, was washed with PBS and trimmed into approximately 15x15cm^2 portions. Membrane portions were kept in a decellularization solution (0.1% sodium dodecyl sulfate, SDS, Affymetrix USB, Cleveland, USA) for at least 24 hours on a horizontal mechanical shaker at room temperature (RT) at approximately 120rpm, followed by gentle scraping with cell scraper over sterile silicone mat. The decellularization process was confirmed with histochemical staining with 0.4% Trypan Blue, which stains dead cells. Membrane decellularization and cell cultivation onto DAM discs were also observed after histological preparation of cross-section: fixation with 10% natural buffered formalin, dehydration through increasing series of graduated ethanol, embedding in paraffin wax, sectioning at 4 μm thickness, and staining with by Haematoxylin and Eosin (H&E). The decellularized membranes were washed five times with PBS at RT and stocked in PBS at 4°C. Membranes were rewashed, cut into circles with an 8mm diameter surgical punch (Golgran, São Caetano do Sul, Brazil), stretched on culture dishes, kept with PBS exposed to UV light for 1 hour inside the laminar flow, and incubated in complete culture medium in standard culture conditions of 5% CO2 in air at 37°C without cells for 72h. Adipose-derived stromal cells were collected from the inguinal fat of two eight-week-old male Wistar rats after the animals were anesthetized by intraperitoneal administration 50 mg/Kg ketamine (Dopalen, Vetbrands; Paulínia, Brazil) and 6,6 mg/Kg xylazine (Anasedan, Vetbrands; Paulínia, Brazil).

Intracardiac administration of Thiopental 75 mg/kg (Tiopentax, Cristália; Itapira, Brazil) was used for animal euthanasia. The SVF was obtained by collagenase digestion, according to previously published methods [30]. Adipose tissue was washed with PBS, macerated with two n.22 surgical blades, digested for 30 minutes at 37°C in PBS containing 0.075% collagenase type I (GIBCO Life Technologies; Rockville, USA). Digested tissue was centrifuged at 1.200rpm for 10 minutes after adding complete culture medium: Dulbecco's modified Eagle's medium-F12 (Sigma-Aldrich; St Louis, USA), supplemented with 10% fetal bovine serum (FBS, GIBCO Life Technologies; Rockville, USA) and 1% streptomycin/penicillin. Cells were suspended in PBS, passed in a 100μm strainer (Becton Dickinson; Franklin Lakes, USA), and centrifuged before suspension in the supplemented medium. Nucleated cell yield was verified in a hemocytometer after Trypan Blue staining, and the initial plating density was 1×10^5 cells/cm^2 in T25 culture flasks. Cell culture flasks were incubated at 37°C in a humidified atmosphere with 5% CO2 atmosphere. Nonadherent cells were removed after 72 hours, and adherent cells were maintained, with a medium change every three days. Upon reaching 80% confluency, ASCs were transferred to another flask/dish after incubation with 0.25% trypsin/0.1% EDTA (Cellgro; Manassas, USA), expanded from a plating density of 1×10^3 cells/cm^2 in T75 culture flask in the second passage, and cryopreserved in 80% FBS, 10% medium, 10% dimethyl sulfoxide (DMSO, Sigma-Aldrich; Saint Louis, USA). Cryopreserved ASCs were extracted from liquid nitrogen, rapidly thawed in a culture medium, centrifuged at 1.200rpm for 10 min, the supernatant was discarded, and the pellet was resuspended in a complete culture medium. Cells (at the third passage) were cultivated onto polystyrene dishes and on DAM at a density of 1.5×10^4 cells/cm-2 for proliferation. Trilineage differentiation test [57] of the ASCs into Osteoblasts, Chondroblasts, and Adipocytes was examined, after observing their high self-renewal capacity. Cells were maintained on regular medium, and osteoinduction media was used for osteogenic differentiation.

Posted on Authorea 31 Jul 2020 — CC0 1.0 — https://doi.org/10.22541/au.159620994.43378706 — This a preprint and has not been peer reviewed. Data may be preliminary.

Two different osteoinduction media were used separately after cell confluence. Osteogenic induction medium was prepared with reagents known to favor the expression of the osteoblastic phenotype: 50mcg/mL Ascorbic acid (Sigma-Aldrich, Tokyo, Japan), 10mM β-Glycerophosphate (Sigma-Aldrich, St. Louis, USA), and 100nM dexamethasone (Sigma-Aldrich, St. Louis, USA) diluted in regular supplemented medium. The commercially available Rat Osteoblast Differentiation Medium (Cell Applications, Inc; San Diego, USA) was also used. Either medium was added after cell confluence and changed every 3 days, up to 4 weeks of culture. Mineralization was observed by histochemical staining with Alizarin red staining (affinity for calcium) after fixation in 2.5% glutaraldehyde for 1h RT, washing 3 times with 70% ethanol, staining with 1% Alizarin red solution pH 5.5 for 5 min at RT, washing 3 times with 50% ethanol, and air-drying. The cultures were examined under a phase contrast microscope (Zeiss Axio Vert.A1, Zeiss; Jena, Germany), also equipped with an AxioCam MRC camera (Zeiss, Germany).

Chondrogenic Differentiation Medium (Gibco; Carlsbad, USA) was used to differentiate ASCs into chondrocytes after the culture of cell micromass in quadruplicate in a 12-well plate. Cells were centrifuged at 1.200rpm for 10min, resuspended in a regular medium at a cell density of $1.6x10^7$ cells/ml, cultured in a single drop of cell pellet at the center of each well, and incubated for 2 hours; before adding the chondrogenic differentiation medium or regular complete medium, as control. Culture media were exchanged every 72 hours for three weeks of culture. Histochemical coloration with 0.4% Alcian Blue 8GX (Sigma-Aldrich, Saint Louis, USA) was used to demonstrate chondrogenic differentiation, by its affinity with sulfated proteoglycans under acidic conditions. After washing with PBS 37°C, fixation with 2.5% glutaraldehyde for 1 hour, and washing for fixative removal, staining was performed with Alcian Blue solution for 30 minutes, followed by two washes with 0.1N HCl, and wells were kept in distilled water.

The adipogenic differentiation of the ASCs was performed after cell culture in quadruplicate in a 12-well plate reached 80% confluence. Adipogenic differentiation medium was prepared at the time of medium exchange with the addition of 0.5µM dexamethasone, 0.5mM of isobutylmethylxanthine, and 50µM of indomethacin (all from Sigma-Aldrich, Saint Louis, USA) to complete medium, and filtered on 0.22µm membrane. Culture media, differentiation, and control were exchanged every 72 hours for two weeks. Histochemical coloration with Oil Red (Sigma-Aldrich, Saint Louis, USA) was used to demonstrate adipogenic differentiation, by its lipid affinity. After washing with PBS 37°C, fixation with 2.5% glutaraldehyde for 1 hour at room temperature, removal of the fixative, washing with distilled water, and washing with 60% isopropanol for 5 minutes, staining was performed with Oil Red solution by 5 minutes. The dye solution was removed, and wells were washed and kept with distilled water. DAM discs used for animal treatment were cut with an 8mm punch onto a silicon surface.

Cells were cultivated over the DAM discs ($2.5x10^4$cells/cm^2) stretched onto 12-well plates. After cell confluence was observed on the polystyrene area around the membrane discs, in approximately five days, more cells were associated with the discs ($2.5x10^4$ cells/cm^2), 48 hours before the surgical procedure. Fifteen Male Wistar rats (8 weeks old, medium weight 370g) were randomly divided into three treatment groups: no DAM scaffold (T0= control), DAM scaffold only (T1), and DAM scaffold associated with ASCs (T2). The animals were anesthetized as described before. The hair over the cranial bones was shaved, and the skin was aseptically prepared using 70% alcohol scrub. The animal head was stabilized in a stereotaxic frame (Stoelting Co.; Wood Dale, USA) to maintain immovable during surgery.

A sagittal incision was made with a surgical blade through the skin over the calvaria, subcutaneous tissues were divulged, and the area was maintained exposed using an Alm tissue retractor. The anatomic landmarks, sagittal, coronal and lambdoid sutures, were identified, and the periosteum was incised and elevated with a blunt spatula. Non-healing "critical-sized" calvarial defects involved the bones parietal, frontal and occipital, as previously described [58]. A single bicortical full-thickness defect was prepared on the midline using a low-speed dental surgical drilling unit (NSK 20:1 SMax SG20, Tochigi, Japan; Beltec LB 100, Araraquara, Brazil), with an 8 mm diameter trephine (Neodent; Curitiba, Brazil). Care was taken to avoid injury to the dura mater, with intermittent movement, and constant irrigation with saline solution. After the calvarial bone disc removal, the area was cleaned with abundant irrigation before the treatment. Four layers of DAM

Posted on Authorea 31 Jul 2020 — CC0 1.0 — https://doi.org/10.22541/au.159620994.43378706 — This a preprint and has not been peer reviewed. Data may be preliminary.

(T1) or four layers of DAM with ASCs (T2) were placed stretched one over one another on the dura, which was maintained intact at the defect base, without extending beyond the defect margins. The implants were maintained in place with the overlying periosteum. The subcutaneous tissue was approximated, and the surgical site was closed primarily using a 7.0 polypropylene suture (Ethicon/Johnson & Johnson; São Paulo, Brazil). Analgesic was administered for three days following the surgery. Euthanasia of the animals with the same procedure described, after 12 weeks of bone repair, was followed by specimen excision with a diamond disc, and one week of fixation with 10% natural buffered formalin. The excised specimens were scanned with a SkyScan1174v2 Micro-computed tomography (micro-CT) scanner (50Kv, 800μA, pixel size 16.82μm; Bruker micro-CT, Kontich, Belgium). Micro-CT images were reconstructed, aligned, visualized, and measured (Softwares NRecon, DataViewer, CTVox, and CTAn; Bruker micro-CT, Kontich, Belgium). For the measurement of various parameters with CTAn, a cylindrical ROI (9.3mm in diameter) was placed on the center of the defect on a 2D image, enclosing all the new bone within the defect, and the defect margin. Measurement was done on 30 layers comprising the tridimensional defect volume after demarcating a threshold value from the gray level histogram. The following basic parameters were measured: Bone volume, Percentage of new bone volume in the total tissue volume (BV/TV), and Trabecular number.

The specimens were decalcified with 10% EDTA (Ethylenediaminetetraacetic acid solution, pH 7.4) for three weeks, embedded in paraffin, and 4μm histological sections were prepared, perpendicular to the sagittal suture. Deparaffinized sections were stained using H&E (Alcoholic solution, Biotec; Pinhais, Brazil) for baseline observation, and Picrosirius red stain (PRS, Direct Red 80, Sigma-Aldrich; Milwaukee, USA), observed under linearly polarized light (POL). The PSR-POL method was used for morphometric image analysis of fifteen consecutive fields from a histological section of the central area of three specimens of each group. The collagenous content on the defect thickness was measured, including the periosteal and the meningeal sides. Images were captured with an AxioCam MRc digital camera attached to a microscope (Zeiss, Göttingen, Germany; Software AxioVision SE). Image analysis was performed with the software Image-Pro Plus 7.0 (Media Cybernetics, Inc., Rockville, USA), quantifying the total polarized fiber content against the dark background.

Statistical analysis was performed after the Shapiro-Wilk test for normality, using ANOVA along with post hoc Tukey's test, or with nonparametric test Kruskal-Wallis (STATISTICA software, Version 10, StatSoft Inc., USA). Results were presented as the Mean ± Standard Deviation (SD), where $*p < 0.05$ was considered significant.

RESULTS

The decellularization process with 0.1% SDS, after separation from the chorion, was effective in removing the innermost epithelial layer of cells, which lies adjacent to the fetus (Figure 1A). The structure of the subjacent collagenous layer was preserved after decellularization (Figure 1B), as a translucent acellular framework. The DAM preserved its structural integrity during the decellularization, and throughout the cell culture with regular medium, and both osteoinduction media evaluated.

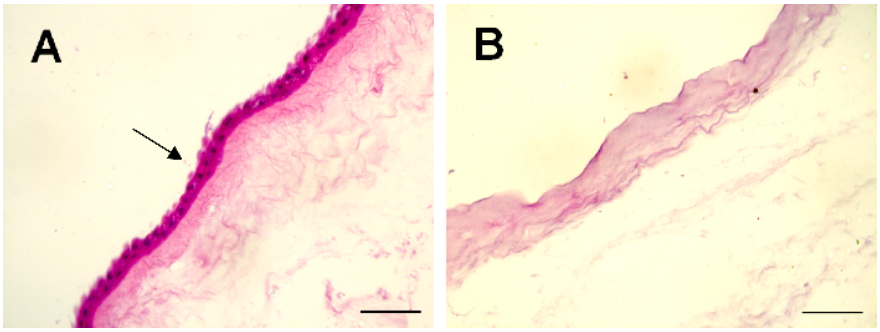

Figure 1. Cross-sections of the human amniotic membrane. The fresh and intact amniotic membrane before

Posted on Authorea 31 Jul 2020 — CC0 1.0 — https://doi.org/10.22541/au.159620994.43378706 — This a preprint and has not been peer reviewed. Data may be preliminary.

decellularization presented the epithelial layer (arrow, A). The decellularization process was effective in removing the epithelial cell layer and preserved the membrane matrix (B). H&E stain, Objective 20X, Scale bars 100 μm.

ASCs with a density of 1.5×104 cells/cm^{-2} adhered and proliferated in culture on all tested substrates and reached confluence in about four days. Cell distribution on the DAM was not easy to distinguish during culture than on polystyrene dishes (Figure 2A). Cells on the DAM cultivated with regular proliferation medium remained most on the surface of the membrane and kept a more elongated, fibroblastic-like shape (Figure 2B). The osteoinduction of ASCs on polystyrene and DAM promoted cell shape alteration to a more polygonal shape, associated with the deposition of the extracellular matrix, also observed as nodular accretions on these substrates (Figures 2C-2F). Both osteoinduction media stimulated the formation of matrix indicated by the osteogenically differentiated ASCs and nodular accretions, first observed after 2 or 3 weeks, and increased until culture termination at four weeks. Mineralized deposits were observed only in the presence of osteoinduction media, as bright red nodules after Alizarin red staining (Figures 2C-2F). Mineralized matrix deposition by the ASCs associated with the DAM was evenly distributed throughout the DAM (Figures 2D, 2F), but on polystyrene was dispersed, in a patchy configuration (Figures 2C, 2E).

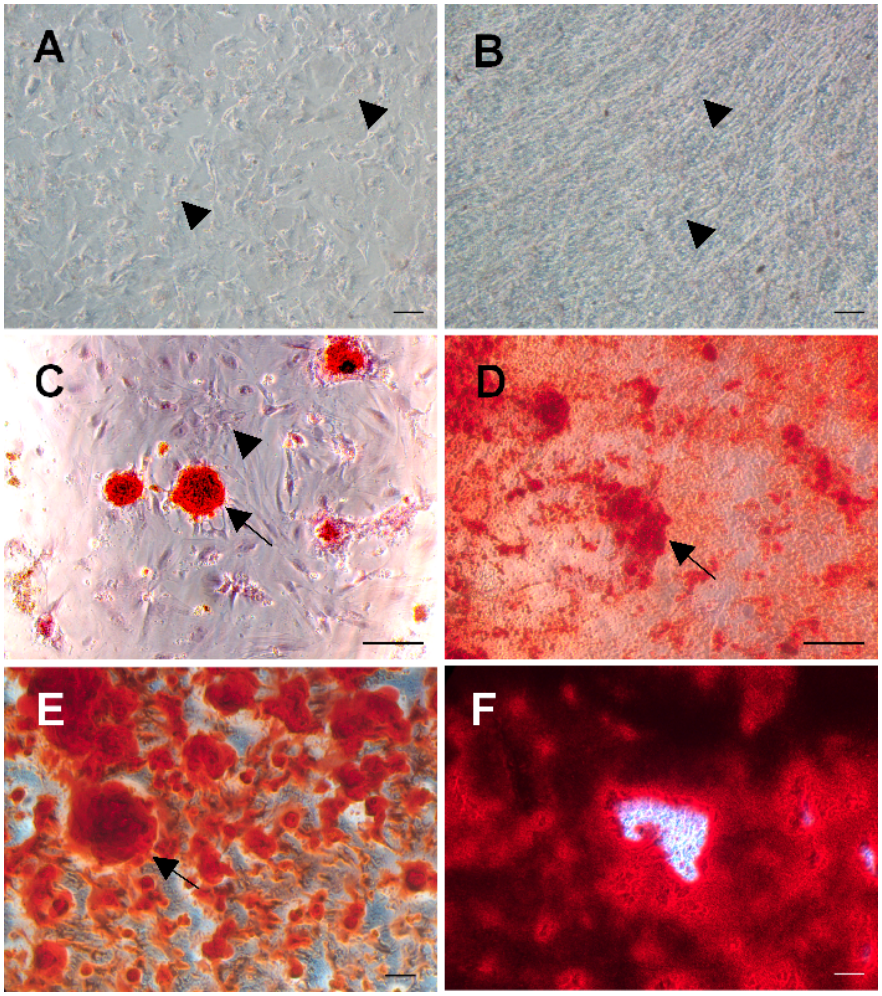

Figure 2. Representative areas of ASCs cultures for four weeks demonstrated osteogenic differentiation. Cultures with the standard medium on polystyrene (A) and membrane (B) present cells (arrowhead) distributed

Posted on Authorea 31 Jul 2020 — CC0 1.0 — https://doi.org/10.22541/au.159620994.43378706 — This a preprint and has not been peer reviewed. Data may be preliminary.

on the dish and the membrane, without mineral deposits. Both osteoinduction media, prepared (C, D), and commercial (E, F), stimulated the deposition of a mineralized matrix, (arrow, red) on polystyrene (C, E) and the membrane (D, F). Alizarin Red stain; Objectives 10X (A, B, E, F), 20X (C, D); Scale bars 100 μm.

Chondrogenic differentiation was observed with the deposition of the proteoglycan-rich matrix on ASCs micromasses cultivated for three weeks with commercial chondrogenic differentiation medium (Figure 3A). The presence of multiple intracellular lipid droplets indicated adipogenic differentiation, by two weeks post-induction with prepared adipogenic differentiation medium (Figure 3C).

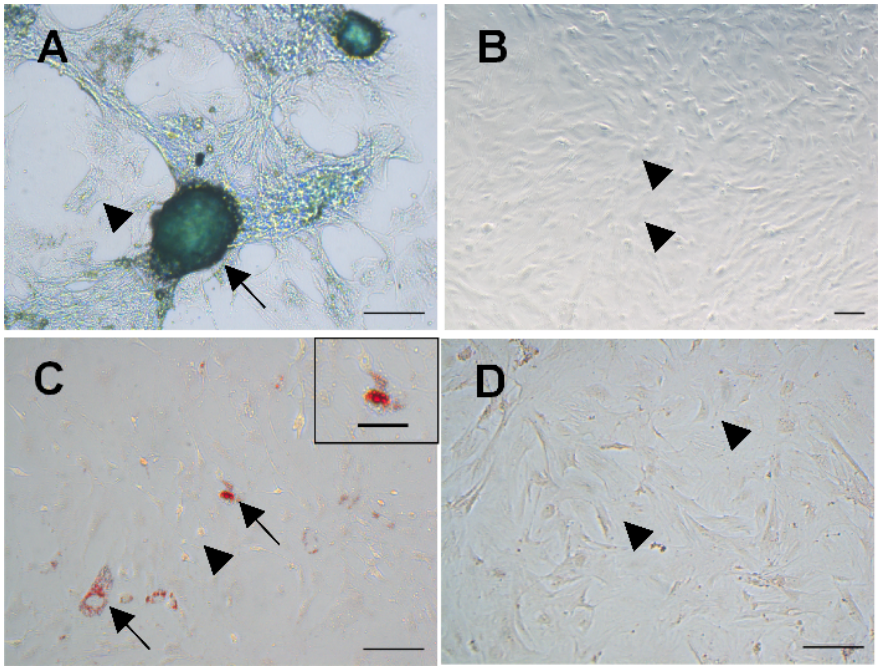

Figure 3. ASCs multilineage differentiation demonstrated by the presence of sulfated proteoglycans on ASCs micromass (A, arrow) and intracellular lipid-filled vacuoles after culture with chondrogenic and adipogenic induction media (B), respectively. ASCs maintained in control medium were processed as negative controls, for chondrogenic (B) and adipogenic (D) differentiation. Alcian Blue stain (A, B); Oil-red stain (C, D); Objectives 10X (B), 20X (A, C, D); Scale bars 100 μm (A-D), 50 μm (inset in C).

Analysis of the *micro-CT images* revealed bone formation at the site of the defects in all three groups observed, from adjacent native bone. A centripetal *in vivo* ossification pattern was observed with bone deposition from and higher on the defect margins. Bone deposition closer to the defect central area was observed in defects with membrane or membrane associated with cells (Figure 4), without complete bony bridging.

Posted on Authorea 31 Jul 2020 — CC0 1.0 — https://doi.org/10.22541/au.159620994.43378706 — This a preprint and has not been peer reviewed. Data may be preliminary.

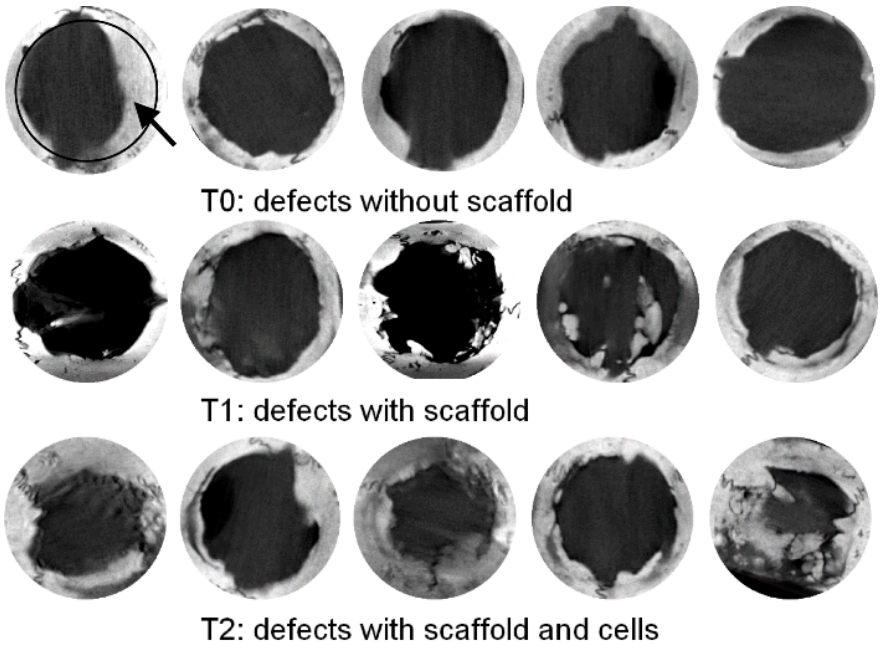

Figure 4. Micro-computed tomography (micro-CT) imaging of rat calvarial defects after 12 weeks of healing, with different treatments. Images of the defects, without scaffold (control, T0), treated with decellularized amniotic membranes (DAM, T1) and DAM with Adipose-derived stromal cells (DAM + ASCs, T2). Bone (arrow) deposited from the defect margins (dotted line, first picture) towards the center. The original defect size with 8mm in diameter, circular images (10mm in diameter).

The *statistical analysis of calvarial bone healing parameters from micro-CT* revealed significant difference on percentage of new bone volume to total bone (BV/TV), and trabecular number. The significant increase in bone volume percentage was observed with the treatment with DAM associated with ASCs (T2= 41.59 ± 11.72), compared to control (T0= 22.85 ± 3.46), but not with DAM alone (T1= 25.95 ± 2.26). The higher repair observed in DAM grafted defects was evidenced by a significantly higher number of trabeculae (mm) in treatment with DAM associated with ASCs (T2 = 1.07 ± 0.35), compared to control T0 (0.61 ± 0.12), but without difference to implanted DAM in T1 (0.82 ± 0.09).

Histological analysis with H&E (Figure 5, Figure 6) and PCR staining (Figure 7) confirmed Micro-CT findings. Collagen organization in the defect area was evaluated by PRS-POL, where collagen appears bright red, yellow, or green, in sharp contrast with the rest of the tissue that remains dark (Figure 7). Defects without treatment presented less bone deposited at the defect margins, and it merged with a thin fibrous host periosteum and the connective tissue layer covering the inner area of the defect, characteristic of defect healing with less bone tissue repair (Figure 5C). The fibrous tissue covering the central part of the defect was thinner than the original well-vascularized bone tissue in the absence of membrane, with a connective tissue collapse observed in untreated defects. The effect of the DAM scaffold on osteoconduction was observed by providing anchorage for bone tissue deposited in the defects (Figure 5).

Posted on Authorea 31 Jul 2020 — CC0 1.0 — https://doi.org/10.22541/au.159620994.43378706 — This a preprint and has not been peer reviewed. Data may be preliminary.

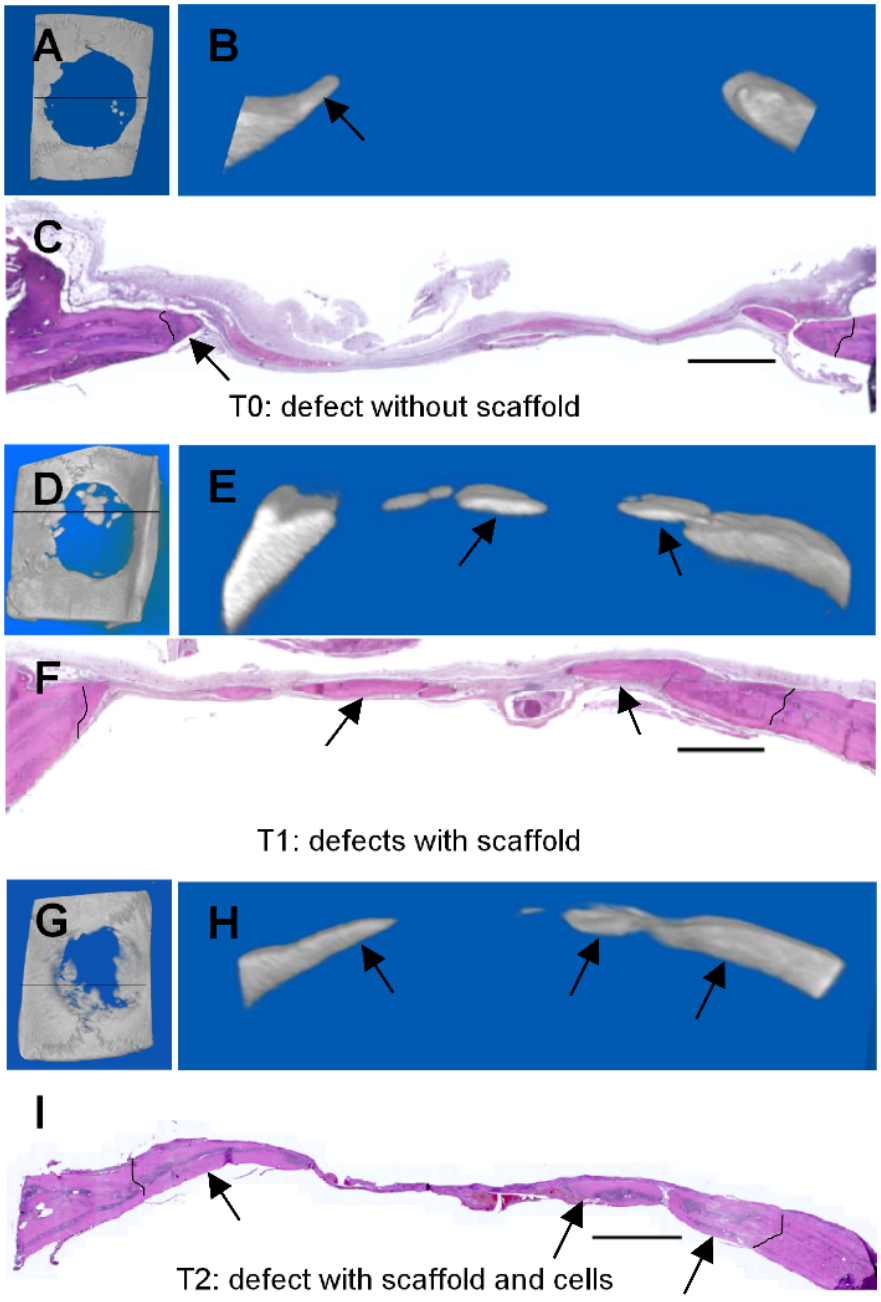

Figure 5. Bone repair of calvarial defects: without treatment (T0, A, B, C), treatment with DAM scaffold (T1, D, E, F), and with DAM associated with transplanted ASCs (T2, G, H, I). Correspondence of images from defect micro-CT of the complete defect (A, D, G) with frontal view position indicated (continuous line), frontal plane (B, E, H), and the histological section of the same area from micro-CT (C, F, I) with the meningeal side towards the bottom of the section. Bone deposition (arrows) from original defect edges (dotted lines) following the periosteum and the collagenous scaffold. H&E stain; Scale bars 1000 μm.

Cortical bone tissue deposited in calvarial defects treated with DAM, such as margin extensions or islets, had amniotic membrane-embedded or as a lining (Figure 6). Newly formed bone from the margins of

Posted on Authorea 31 Jul 2020 — CC0 1.0 — https://doi.org/10.22541/au.159620994.43378706 — This a preprint and has not been peer reviewed. Data may be preliminary.

defects treated with membranes followed the scaffold orientation towards the center of the defect (Figures 5, 6). Remnants of the decellularized amniotic membrane were observed in both membrane treatments as a homogeneous fibrous material, restricted into the defect and, maintained the integrity during the observation period without stimulation of inflammatory and immune response.

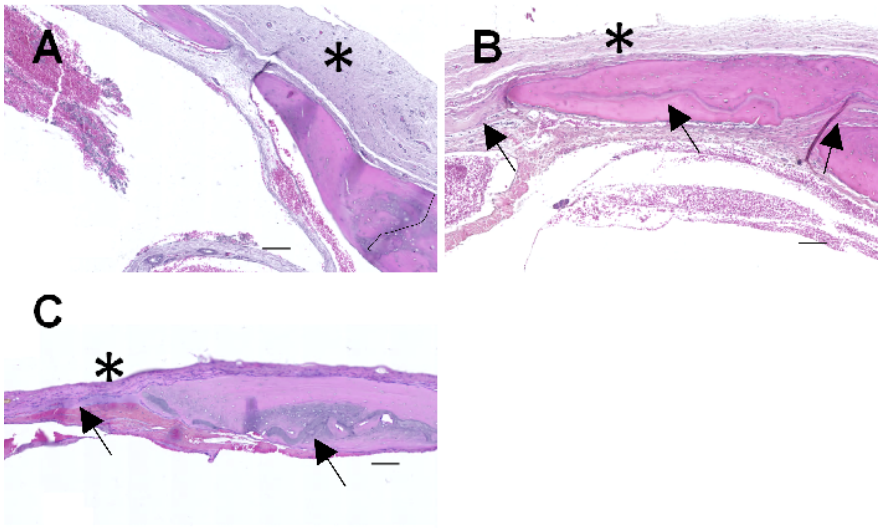

Figure 6. Details of bone deposition from specimens without treatment (T0, A), treatment with DAM scaffold (T1, B), and with DAM associated with transplanted ASCs (T2, C). Bone deposited onto the defect margin (dotted line) associated with the inner cambium or osteogenic layer of the host periosteum, adjacent to its fibrous layer (asterisk) (A). Osteoconduction with DAM layers (arrow) observed adjacent to newly deposited bone, inserted into the bone matrix, and associated with the inner periosteum layer towards the center of the defect (asterisk) (B). Osteoconduction with DAM and ASCs, with DAM scaffold inserted into the bone (arrow) and associated with periosteum (asterisk). H&E s; Objective 2.5X; Scale bars 100 μm.

DAM scaffold enabled the ingrowth of vessels, stem cells, and osteoblasts from the host bone (Figure 7). Collagenous niches for osteogenesis were observed on DAM concave areas from slightly undulated membrane scaffolds (Figure 7) and vascularized connective tissue with endogenous cells propagated between the DAM layers or penetrated between the collagenous matrix, which provided expanded collagenous niches for osteoconduction and DAM incorporation into newly deposited bone (Figure 7B-7C).

Statistical analysis of the total fiber quantification from consecutive PSR-POL images of different treatments demonstrated a significant increase of fiber content between both DAM treatments (T2= 30.73 ± 12.84; T1= 34.21 ± 15.04) and control (T0= 23.08 ± 17.13). The amniotic membrane layers preserved the thickness of the defect space, more comparable to the uninjured bone than defect without DAM (Figure 7D-7F), regardless of whether they were associated with ASCs or not.

Posted on Authorea 31 Jul 2020 — CC0 1.0 — https://doi.org/10.22541/au.159620994.43378706 — This a preprint and has not been peer reviewed. Data may be preliminary.

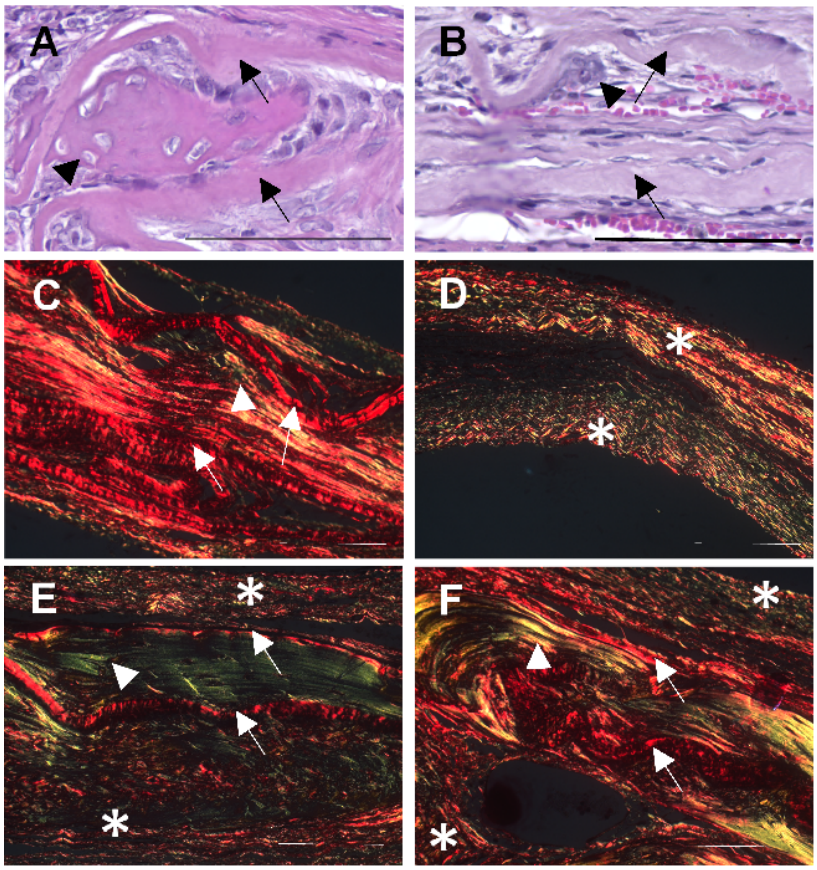

Figure 7. Detail of DAM scaffold in calvarial bone repair. Bone (arrowhead) deposited in the concave area between two transplanted DAM layers (arrow) (A). Osteoconduction established by vascularization between amniotic membrane layers (arrows), cell migration between collagenous fibers of the amniotic membrane, and creation of niches for intermembranous bone deposition (arrow) (B). Picrosirius-polarized image of the specimen from Figure B exhibits the DAM as bright red fiber agglomerate (arrow), interposed by bright yellow endogenous collagen (arrowhead) (C). Picrosirius-polarized images of specimens from three groups: i) without treatment (D, T0), ii) treatment with DAM scaffold (E, T1), and iii) with DAM associated with transplanted ASCs (F, T2), with the meningeal side towards the bottom of the section. Endogenous fibrous tissue from T0 (D), displaying upper and lower parts collapsed (asterisk), without matrix in the middle. Treatments with DAM (T1, E; T2, F) exhibit the transplanted collagenous DAM as bright red fiber agglomerate (arrow) interposed between upper and on lower fibrous tissue (asterisk), and bright green/ yellow endogenous collagen and bone (arrowhead) deposited in the middle. H&E stain (A, B), Picrosirius Red stain (C, D, E, F); Objective 20X (A, B), Objective 10X (C, D, E, F); Scale Bars 100 μm.

DISCUSSION

In the present work, it was applied a combined transplantation approach using ASCs and DAM, and obtained exciting results demonstrating enhanced calvarial bone regeneration. The decellularization process preserved the membranous structure of the amniotic membrane, and the analysis confirmed the absence of deleterious effect of the decellularization on the ultrastructural characteristics of DAM compared to intact amniotic

Posted on Authorea 31 Jul 2020 — CC0 1.0 — https://doi.org/10.22541/au.159620994.43378706 — This a preprint and has not been peer reviewed. Data may be preliminary.

membrane [16]. The cell culture on the decellularized amniotic membrane provides a more biomimetic niche than the culture dish surface [59]. The decellularization method used in the present study ensured membrane biocompatibility, stability during the extended *in vitro*culture period for ASCs osteoblastic differentiation, and preservation of the collagenous matrix integrity, which was not fragile or difficult to handle. Four DAM layers made it possible to cover the entire inner calvarial defect perimeter, increasing the scaffold thickness, replicating the use of multilayered cell sheets [60] when the DAM was associated with ASCs.

These results revealed that the scaffold created by the layers of DAM provided an osteoconductive extracellular matrix environment for the cells during tissue regeneration. The collagenous matrix from the DAM scaffold was incorporated concomitant with host bone deposition, without inducing an inflammatory and immune response, or presenting accelerated scaffold biodegradation. One response to the DAM was osseointegration, with direct bone deposition onto the scaffold, creating a mineralized interface between DAM and newly deposited bone. Another response to the DAM scaffold was "osseointegration", with the inclusion of the collagenous DAM as part of the newly deposited bone.

There are controversial opinions regarding scaffold degradation, with fast degradation *in vitro* contraindicating their use for cell transplantation [61], because prolonged stability is necessary for cell support [62], *versus* rapid degradation as advantageous for cell release in the early period of osseous defect repair [63].

ASCs exhibited multilineage potential demonstrated by the trilineage capacity to differentiate: chondrogenic, osteogenic, and adipogenic lineages. Stem cell participation on bone tissue regeneration may depend on cell attachment and proliferation on scaffolds, subsequent differentiation, and integration into the surrounding tissues [16].*In vitro* results demonstrated ASCs' attachment, cell proliferation, and osteogenic differentiation on DAM.

The association of ASCs with Platelet-Rich Plasma (PRP) increased cellular secretion of growth factors *in vitro* , and bone healing in calvarial defects [64]. However, the association of ASC to non-activated PRP presented no additional positive effect on calvarial defect bone healing [65, 66]. We observed neovascularization of the defect adjacent to the decellularized amniotic membrane, surrounded by endogenous periosteal cells, promoting osteoconduction. Endogenous periosteal cell migration for bone deposition also needs stability for bone deposition. The support provided by the DAM scaffold stimulated osteogenesis by providing a collagenous surface for cell attachment, differentiation into osteoblasts, and deposition of a mineralized matrix, as observed between the DAM layers and between the DAM collagenous matrices.

Intramembranous bone deposition followed two different patterns in the presence of the DAM, depending on the amniotic membrane aspect and their collagenous fibers looseness. Support for vascularization between the collagenous fibers of the amniotic membrane was observed on looser collagenous fibers of the DAM. Undulated DAM was also observed inside lamellar bone deposits. The formation of concave niches for initial islet bone deposition, with subsequent incorporation into the lamellar bone, demonstrated the osteogenic potential of these areas. Previous reports documented those scaffold concavities are conducive for osteogenesis [67, 68].

Quantification of total collagen, from DAM scaffold and endogenous origin, and characterization of the collagen structure was done after PSR-POL, without distinguishing their type or origin, since the orientation, thickness, and packing of collagen bundles determine the amount of polarized light absorbed by the stain [69, 70]. Mature and arranged collagen fibers appear greenish-yellow, and immature collagen in primary bone red-orange [70, 71]. The significant increase of collagen content provided by DAM treatments provided the scaffold to support vascular growth into the defect and osteoconduction.

One limitation of the present study was the lack of cell marker for tracking transplanted cell fate and identification of cell participation in the healing process, if through their intrinsic ability to differentiate into osteoblasts. Even though the contribution of the ASCs for bone healing was not established, this data demonstrated higher repair of critical-size bone defects with transplanted cells and emphasized the indication of the scaffolds prepared with DAM and ASCs in bone tissue engineering. Transplanted ASCs in bone sites may be differentiated into osteoblasts or stimulate endogenous healing by trophic function [72]. New bone in

Posted on Authorea 31 Jul 2020 — CC0 1.0 — https://doi.org/10.22541/au.159620994.43378706 — This a preprint and has not been peer reviewed. Data may be preliminary.

calvarial defects were determined to consist mainly of transplanted cells [48], and ASCs directly differentiated into osteogenic cells *in vivo* [64, 73].

Monolayers or cell sheets can be prepared with cells and cellular matrix, and are alternatives for autologous or allogeneic transplantation, whether or not associated with membranes or scaffolds, and can stimulate osteogenesis and neovascularization [10, 74-76]. A tridimensional cell sheet strategy with the layers of DAM associated with ASCs placed directly to the host site with minimal cell manipulation improved the bone regeneration potential with more vessel stability than single-cell sheet [10].

Osteogenesis through the osteoconduction process, providing a structural scaffold to support vascularization and host cell reconstruction, can explain the successful bone augmentation observed on DAM. Furthermore, the association with ASCs may have allowed osteogenesis through site osteoinduction, observed by the significantly higher bone deposition with DAM and ASCs grafts. The role of the anatomical defect region was determinant for the results obtained in the present study. The calvarial bone defect model, as an orthotopic non-load bearing site, provided an appropriate osteogenic environment to assess the effect of non-induced ASCs for bone tissue engineering [48, 77]. Accelerated bone healing of calvarial defect has been reported in other studies with ASCs, associated with commercial bone graft in rabbit [78], with PLGA/HA [43, 48], and starch-polycaprolactone [79]. Other investigators also observed significant healing improvement with ASCs without previous cell induction, genetic manipulation, or association with exogenous growth factors [45, 48, 72, 80-82]. Untreated ASCs as control also stimulated healing [41, 49, 72, 83]. Osteoinduction of ASCs has been investigated in calvarial bone healing models [8, 52, 84], besides cell transfection with vascular endothelial growth factor (VEGF) gene sequence [49], and cell transduction for sustained expression of BMP and Stromal cell-derived factor[85].

The pro-osteogenic paracrine effect of ASCs was identified between transplanted ASCs and host osteoblasts, through BMP and Hedgehog signaling [47], stimulating the endogenous healing response. ASCs may also accelerate new bone formation by promoting angiogenesis through pro-angiogenic paracrine factors [52, 86-88], and secretion of VEGF [87, 89]. ASCs may participate directly in vasculogenesis, stabilizing endothelial networks by developing pericyte characteristics [86]. Strategies to stimulate bone regeneration are the selection of perivascular cell subsets from SVF [9, 40], and ASCs–derived exosomes [90]. The extended clinical therapeutic use of ASCs for bone regeneration still requires a standard for cell characterization and culture [91].

CONCLUSION

DAM confirmed potential and efficacy for ASCs transplantation in the bone tissue engineering model. *In vivo* DAM treatments demonstrated osteoconduction, providing a collagenous structural matrix for endogenous cell migration, neovascularization, bone tissue deposition, and anchorage. Bone deposited between the DAM layers, especially on niches formed by membrane undulation, or between the collagenous fibers of the DAM, incorporating the DAM into the newly deposited tissue.

The further association of DAM with ASCs, stimulated the healing of critical-sized adult rat calvarial defects, by promoting demonstrated DAM graft incorporation concomitant with higher host bone deposition, compared with defects without treatment. This association of the ASCs and DAM offers advantages for optimizing bone regeneration in this model.

Futures research will be necessary with the association of bioactive materials and in different defect models since DAM with ASCs may also be used for supporting vascularization, periosteal cell migration, and bone healing with implants, even in load-bearing defects.

CONFLICT OF INTEREST

The authors indicated no potential conflicts of interest.

REFERENCES

Posted on Authorea 31 Jul 2020 — CC0 1.0 — https://doi.org/10.22541/au.159620994.43378706 — This a preprint and has not been peer reviewed. Data may be preliminary.

1. Dimitriou R, Jones E, McGonagle D, et al. Bone regeneration: current concepts and future directions. *BMC medicine* 2011; 9: 66.

2. Dimitriou R, Mataliotakis GI, Calori GM, et al. The role of barrier membranes for guided bone regeneration and restoration of large bone defects: current experimental and clinical evidence. *BMC medicine*2012; 10: 81.

3. Konofaos P, Petersen D, Jennings JA, et al. Evaluation of Amniotic Multipotential Tissue Matrix to Augment Healing of Demineralized Bone Matrix in an Animal Calvarial Model. *The Journal of craniofacial surgery* 2015; 26: 1408-1412.

4. Lin Y, Wang T, Wu L, et al. Ectopic and in situ bone formation of adipose tissue-derived stromal cells in biphasic calcium phosphate nanocomposite. *Journal of biomedical materials research Part A*2007; 81: 900-910.

5. Hosseinpour S, Ghazizadeh Ahsaie M, Rezai Rad M, et al. Application of selected scaffolds for bone tissue engineering: a systematic review.*Oral and maxillofacial surgery* 2017; 21: 109-129.

6. Lappalainen OP, Korpi R, Haapea M, et al. Healing of rabbit calvarial critical-sized defects using autogenous bone grafts and fibrin glue.*Childs Nerv Syst* 2015; 31: 581-587.

7. Lappalainen OP, Haapea M, Serpi R, et al. Iron-labeled adipose stem cells and neovascularization in rabbit calvarial critical-sized defects.*Oral surgery, oral medicine, oral pathology and oral radiology*2016; 121: e104-110.

8. Dudas JR, Marra KG, Cooper GM, et al. The osteogenic potential of adipose-derived stem cells for the repair of rabbit calvarial defects.*Ann Plast Surg* 2006; 56: 543-548.

9. Wang Y, Xu J, Chang L, et al. Relative contributions of adipose-resident CD146(+) pericytes and CD34(+) adventitial progenitor cells in bone tissue engineering. *NPJ Regen Med* 2019; 4: 1.

10. Caridade SG, Mano JF. (*) Engineering Membranes for Bone Regeneration. *Tissue engineering Part A* 2017; 23: 1502-1533.

11. Ramalingam S, Al-Rasheed A, ArRejaie A, et al. Guided bone regeneration in standardized calvarial defects using beta-tricalcium phosphate and collagen membrane: a real-time in vivo micro-computed tomographic experiment in rats. *Odontology* 2016; 104: 199-210.

12. Umoh JU, Sampaio AV, Welch I, et al. In vivo micro-CT analysis of bone remodeling in a rat calvarial defect model. *Physics in medicine and biology* 2009; 54: 2147-2161.

13. Al-Hezaimi K, Ramalingam S, Al-Askar M, et al. Real-time-guided bone regeneration around standardized critical size calvarial defects using bone marrow-derived mesenchymal stem cells and collagen membrane with and without using tricalcium phosphate: an in vivo micro-computed tomographic and histologic experiment in rats. *International journal of oral science* 2016; 8: 7-15.

14. Silva-Cote I, Cruz-Barrera M, Canas-Arboleda M, et al. Strategy for the Generation of Engineered Bone Constructs Based on Umbilical Cord Mesenchymal Stromal Cells Expanded with Human Platelet Lysate.*Stem cells international* 2019; 2019: 7198215.

15. Ansari AS, Yazid MD, Sainik N, et al. Osteogenic Induction of Wharton's Jelly-Derived Mesenchymal Stem Cell for Bone Regeneration: A Systematic Review. *Stem cells international* 2018; 2018: 2406462.

16. Salah RA, Mohamed IK, El-Badri N. Development of decellularized amniotic membrane as a bioscaffold for bone marrow-derived mesenchymal stem cells: ultrastructural study. *Journal of molecular histology*2018; 49: 289-301.

17. Niknejad H, Peirovi H, Jorjani M, et al. Properties of the amniotic membrane for potential use in tissue engineering. *Eur Cell Mater*2008; 15: 88-99.

Posted on Authorea 31 Jul 2020 — CC0 1.0 — https://doi.org/10.22541/au.159620994.43378706 — This a preprint and has not been peer reviewed. Data may be preliminary.

18. Zhang C, Yu L, Liu S, et al. Human amnion-derived mesenchymal stem cells promote osteogenic and angiogenic differentiation of human adipose-derived stem cells. *PloS one* 2017; 12: e0186253.

19. Mamede AC, Carvalho MJ, Abrantes AM, et al. Amniotic membrane: from structure and functions to clinical applications. *Cell and tissue research* 2012; 349: 447-458.

20. Francisco JC, Correa Cunha R, Cardoso MA, et al. Decellularized Amniotic Membrane Scaffold as a Pericardial Substitute: An In Vivo Study. *Transplantation proceedings* 2016; 48: 2845-2849.

21. Kubo M, Sonoda Y, Muramatsu R, et al. Immunogenicity of human amniotic membrane in experimental xenotransplantation.*Investigative ophthalmology & visual science* 2001; 42: 1539-1546.

22. Gholipourmalekabadi M, Mozafari M, Salehi M, et al. Development of a Cost-Effective and Simple Protocol for Decellularization and Preservation of Human Amniotic Membrane as a Soft Tissue Replacement and Delivery System for Bone Marrow Stromal Cells. *Advanced healthcare materials* 2015; 4: 918-926.

23. Gholipourmalekabadi M, Sameni M, Radenkovic D, et al. Decellularized human amniotic membrane: how viable is it as a delivery system for human adipose tissue-derived stromal cells? *Cell proliferation* 2016; 49: 115-121.

24. Semyari H, Rajipour M, Sabetkish S, et al. Evaluating the bone regeneration in calvarial defect using osteoblasts differentiated from adipose-derived mesenchymal stem cells on three different scaffolds: an animal study. *Cell and tissue banking* 2016; 17: 69-83.

25. Chen YJ, Chung MC, Jane Yao CC, et al. The effects of acellular amniotic membrane matrix on osteogenic differentiation and ERK1/2 signaling in human dental apical papilla cells. *Biomaterials*2012; 33: 455-463.

26. Iwasaki K, Komaki M, Yokoyama N, et al. Periodontal regeneration using periodontal ligament stem cell-transferred amnion. *Tissue engineering Part A* 2014; 20: 693-704.

27. Wu PH, Chung HY, Wang JH, et al. Amniotic membrane and adipose-derived stem cell co-culture system enhances bone regeneration in a rat periodontal defect model. *Journal of the Formosan Medical Association = Taiwan yi zhi* 2016; 115: 186-194.

28. Akazawa K, Iwasaki K, Nagata M, et al. Double-layered cell transfer technology for bone regeneration. *Scientific reports* 2016; 6: 33286.

29. Fenelon M, Chassande O, Kalisky J, et al. Human amniotic membrane for guided bone regeneration of calvarial defects in mice. *Journal of materials science Materials in medicine* 2018; 29: 78.

30. Zuk P. Adipose-Derived Stem Cells in Tissue Regeneration: A Review.*ISRN Stem Cells* 2013; 2013: 35.

31. Zuk PA. The adipose-derived stem cell: looking back and looking ahead. *Mol Biol Cell* 2010; 21: 1783-1787.

32. Mizuno H, Tobita M, Uysal AC. Concise review: Adipose-derived stem cells as a novel tool for future regenerative medicine. *Stem Cells* 2012; 30: 804-810.

33. Thesleff T, Lehtimaki K, Niskakangas T, et al. Cranioplasty with adipose-derived stem cells and biomaterial: a novel method for cranial reconstruction. *Neurosurgery* 2011; 68: 1535-1540.

34. Mesimaki K, Lindroos B, Tornwall J, et al. Novel maxillary reconstruction with ectopic bone formation by GMP adipose stem cells.*Int J Oral Maxillofac Surg* 2009; 38: 201-209.

35. Khojasteh A, Hosseinpour S, Rad MR, et al. Buccal Fat Pad-Derived Stem Cells in Three-Dimensional Rehabilitation of Large Alveolar Defects: A Report of Two Cases. *J Oral Implantol* 2019; 45: 45-54.

36. Gomes SP, Deliberador TM, Gonzaga CC, et al. Bone healing in critical-size defects treated with immediate transplant of fragmented autogenous white adipose tissue. *The Journal of craniofacial surgery*

Posted on Authorea 31 Jul 2020 — CC0 1.0 — https://doi.org/10.22541/au.159620994.43378706 — This a preprint and has not been peer reviewed. Data may be preliminary.

2012; 23: 1239-1244.

37. Azevedo-Neto RD, Gonzaga CC, Deliberador TM, et al. Fragmented adipose tissue transplanted to craniofacial deformities induces bone repair associated with immunoexpression of adiponectin and parathyroid hormone 1-receptor. *Cleft Palate Craniofac J* 2013; 50: 639-647.

38. Rhee SC, Ji YH, Gharibjanian NA, et al. In vivo evaluation of mixtures of uncultured freshly isolated adipose-derived stem cells and demineralized bone matrix for bone regeneration in a rat critically sized calvarial defect model. *Stem Cells Dev* 2011; 20: 233-242.

39. Todorov A, Kreutz M, Haumer A, et al. Fat-Derived Stromal Vascular Fraction Cells Enhance the Bone-Forming Capacity of Devitalized Engineered Hypertrophic Cartilage Matrix. *Stem cells translational medicine* 2016; 5: 1684-1694.

40. James AW, Zara JN, Corselli M, et al. An abundant perivascular source of stem cells for bone tissue engineering. *Stem cells translational medicine* 2012; 1: 673-684.

41. Yoon E, Dhar S, Chun DE, et al. In vivo osteogenic potential of human adipose-derived stem cells/poly lactide-co-glycolic acid constructs for bone regeneration in a rat critical-sized calvarial defect model. *Tissue Eng* 2007; 13: 619-627.

42. Levi B, James AW, Nelson ER, et al. Studies in adipose-derived stromal cells: migration and participation in repair of cranial injury after systemic injection. *Plastic and reconstructive surgery*2011; 127: 1130-1140.

43. Cowan CM, Aalami OO, Shi YY, et al. Bone morphogenetic protein 2 and retinoic acid accelerate in vivo bone formation, osteoclast recruitment, and bone turnover. *Tissue Eng* 2005; 11: 645-658.

44. Levi B, Nelson ER, Li S, et al. Dura mater stimulates human adipose-derived stromal cells to undergo bone formation in mouse calvarial defects. *Stem Cells* 2011; 29: 1241-1255.

45. Levi B, Nelson ER, Brown K, et al. Differences in osteogenic differentiation of adipose-derived stromal cells from murine, canine, and human sources in vitro and in vivo. *Plastic and reconstructive surgery* 2011; 128: 373-386.

46. Levi B, James AW, Nelson ER, et al. Acute skeletal injury is necessary for human adipose-derived stromal cell-mediated calvarial regeneration. *Plastic and reconstructive surgery* 2011; 127: 1118-1129.

47. Levi B, James AW, Nelson ER, et al. Human adipose-derived stromal cells stimulate autogenous skeletal repair via paracrine Hedgehog signaling with calvarial osteoblasts. *Stem Cells Dev* 2011; 20: 243-257.

48. Cowan CM, Shi YY, Aalami OO, et al. Adipose-derived adult stromal cells heal critical-size mouse calvarial defects. *Nat Biotechnol*2004; 22: 560-567.

49. Kim I, Lee SS, Kim SHL, et al. Osteogenic Effects of VEGF-Overexpressed Human Adipose-Derived Stem Cells with Whitlockite Reinforced Cryogel for Bone Regeneration. *Macromol Biosci* 2019; 19: e1800460.

50. Kim HJ, Park SS, Oh SY, et al. Effect of acellular dermal matrix as a delivery carrier of adipose-derived mesenchymal stem cells on bone regeneration. *J Biomed Mater Res B Appl Biomater* 2012; 100: 1645-1653.

51. Heo SC, Shin WC, Lee MJ, et al. Periostin accelerates bone healing mediated by human mesenchymal stem cell-embedded hydroxyapatite/tricalcium phosphate scaffold. *PloS one* 2015; 10: e0116698.

52. Wang G, Roohani-Esfahani SI, Zhang W, et al. Effects of Sr-HT-Gahnite on osteogenesis and angiogenesis by adipose derived stem cells for critical-sized calvarial defect repair. *Scientific reports* 2017; 7: 41135.

53. Kim JH, Park MH, Jang SJ, et al. Effect of Hydrogen Dioxide Treatment on the Osteogenic Potential of Duck-beak Bone-derived Natural Bioceramic Microparticles. *In vivo* 2017; 31: 373-379.

Posted on Authorea 31 Jul 2020 — CC0 1.0 — https://doi.org/10.22541/au.159620994.43378706 — This a preprint and has not been peer reviewed. Data may be preliminary.

54. Dziedzic DSM, Mogharbel BF, Ferreira PE, et al. Transplantation of Adipose-derived Cells for Periodontal Regeneration: A Systematic Review. *Current stem cell research & therapy* 2018.

55. Rickham PP. Human Experimentation. Code of Ethics of the World Medical Association. Declaration of Helsinki. *British medical journal* 1964; 2: 177.

56. Kilkenny C, Browne WJ, Cuthill IC, et al. Improving bioscience research reporting: the ARRIVE guidelines for reporting animal research. *Osteoarthritis Cartilage* 2012; 20: 256-260.

57. Zuk PA, Zhu M, Mizuno H, et al. Multilineage cells from human adipose tissue: implications for cell-based therapies. *Tissue Eng*2001; 7: 211-228.

58. Cooper GM, Mooney MP, Gosain AK, et al. Testing the critical size in calvarial bone defects: revisiting the concept of a critical-size defect. *Plastic and reconstructive surgery* 2010; 125: 1685-1692.

59. Khalil S, El-Badri N, El-Mokhtaar M, et al. A Cost-Effective Method to Assemble Biomimetic 3D Cell Culture Platforms. *PloS one* 2016; 11: e0167116.

60. Shuai Y, Liao L, Su X, et al. Melatonin Treatment Improves Mesenchymal Stem Cells Therapy by Preserving Stemness during Long-term In Vitro Expansion. *Theranostics* 2016; 6: 1899-1917.

61. Donzelli E, Salvade A, Mimo P, et al. Mesenchymal stem cells cultured on a collagen scaffold: In vitro osteogenic differentiation. *Archives of oral biology* 2007; 52: 64-73.

62. Sugawara A, Sato S. Application of dedifferentiated fat cells for periodontal tissue regeneration. *Human cell* 2014; 27: 12-21.

63. Nunez J, Sanz-Blasco S, Vignoletti F, et al. Periodontal regeneration following implantation of cementum and periodontal ligament-derived cells. *J Periodontal Res* 2012; 47: 33-44.

64. Tajima S, Tobita M, Orbay H, et al. Direct and indirect effects of a combination of adipose-derived stem cells and platelet-rich plasma on bone regeneration. *Tissue engineering Part A* 2015; 21: 895-905.

65. Abdelwahid E, Kalvelyte A, Stulpinas A, et al. Stem cell death and survival in heart regeneration and repair. *Apoptosis* 2016; 21: 252-268.

66. Jeong W, Kim YS, Roh TS, et al. The effect of combination therapy on critical-size bone defects using non-activated platelet-rich plasma and adipose-derived stem cells. *Childs Nerv Syst* 2020; 36: 145-151.

67. Ripamonti U, Herbst NN, Ramoshebi LN. Bone morphogenetic proteins in craniofacial and periodontal tissue engineering: experimental studies in the non-human primate Papio ursinus. *Cytokine & growth factor reviews* 2005; 16: 357-368.

68. Graziano A, d'Aquino R, Cusella-De Angelis MG, et al. Concave pit-containing scaffold surfaces improve stem cell-derived osteoblast performance and lead to significant bone tissue formation. *PloS one* 2007; 2: e496.

69. Lattouf R, Younes R, Lutomski D, et al. Picrosirius red staining: a useful tool to appraise collagen networks in normal and pathological tissues. *The journal of histochemistry and cytochemistry : official journal of the Histochemistry Society* 2014; 62: 751-758.

70. Coleman R. Picrosirius red staining revisited. *Acta histochemica* 2011; 113: 231-233.

71. Mubarak S, Masako N, Al-Omari FA, et al. Effect of Collagen Cross-Link Deficiency on Incorporation of Grafted Bone. *Dent J (Basel)* 2019; 7.

72. Ruetze M, Richter W. Adipose-derived stromal cells for osteoarticular repair: trophic function versus stem cell activity. *Expert Rev Mol Med* 2014; 16: e9.

73. Liu G, Zhang Y, Liu B, et al. Bone regeneration in a canine cranial model using allogeneic adipose derived stem cells and coral scaffold. *Biomaterials* 2013; 34: 2655-2664.

Posted on Authorea 31 Jul 2020 — CC0 1.0 — https://doi.org/10.22541/au.159620994.43378706 — This a preprint and has not been peer reviewed. Data may be preliminary.

74. Fang X, Murakami H, Demura S, et al. A novel method to apply osteogenic potential of adipose derived stem cells in orthopaedic surgery. *PloS one* 2014; 9: e88874.

75. Iwata T, Washio K, Yoshida T, et al. Cell sheet engineering and its application for periodontal regeneration. *J Tissue Eng Regen Med*2015; 9: 343-356.

76. Iwata T, Yamato M, Washio K, et al. Periodontal regeneration with autologous periodontal ligament-derived cell sheets - A safety and efficacy study in ten patients. *Regen Ther* 2018; 9: 38-44.

77. Brocher J, Janicki P, Voltz P, et al. Inferior ectopic bone formation of mesenchymal stromal cells from adipose tissue compared to bone marrow: rescue by chondrogenic pre-induction. *Stem cell research* 2013; 11: 1393-1406.

78. Maglione M, Salvador E, Ruaro ME, et al. Bone regeneration with adipose derived stem cells in a rabbit model. *J Biomed Res* 2018.

79. Carvalho PP, Leonor IB, Smith BJ, et al. Undifferentiated human adipose-derived stromal/stem cells loaded onto wet-spun starch-polycaprolactone scaffolds enhance bone regeneration: nude mice calvarial defect in vivo study. *Journal of biomedical materials research Part A* 2014; 102: 3102-3111.

80. Choi JW, Park EJ, Shin HS, et al. In vivo differentiation of undifferentiated human adipose tissue-derived mesenchymal stem cells in critical-sized calvarial bone defects. *Ann Plast Surg* 2014; 72: 225-233.

81. Streckbein P, Jackel S, Malik CY, et al. Reconstruction of critical-size mandibular defects in immunoincompetent rats with human adipose-derived stromal cells. *J Craniomaxillofac Surg* 2013; 41: 496-503.

82. Wilson SM, Goldwasser MS, Clark SG, et al. Adipose-derived mesenchymal stem cells enhance healing of mandibular defects in the ramus of swine. *J Oral Maxillofac Surg* 2012; 70: e193-203.

83. Di Bella C, Farlie P, Penington AJ. Bone regeneration in a rabbit critical-sized skull defect using autologous adipose-derived cells.*Tissue engineering Part A* 2008; 14: 483-490.

84. Jin Y, Zhang W, Liu Y, et al. rhPDGF-BB via ERK pathway osteogenesis and adipogenesis balancing in ADSCs for critical-sized calvarial defect repair. *Tissue engineering Part A* 2014; 20: 3303-3313.

85. Lo SC, Li KC, Chang YH, et al. Enhanced critical-size calvarial bone healing by ASCs engineered with Cre/loxP-based hybrid baculovirus.*Biomaterials* 2017; 124: 1-11.

86. Rohringer S, Hofbauer P, Schneider KH, et al. Mechanisms of vasculogenesis in 3D fibrin matrices mediated by the interaction of adipose-derived stem cells and endothelial cells. *Angiogenesis*2014; 17: 921-933.

87. Rehman J, Traktuev D, Li J, et al. Secretion of angiogenic and antiapoptotic factors by human adipose stromal cells. *Circulation*2004; 109: 1292-1298.

88. Merfeld-Clauss S, Gollahalli N, March KL, et al. Adipose tissue progenitor cells directly interact with endothelial cells to induce vascular network formation. *Tissue engineering Part A* 2010; 16: 2953-2966.

89. Murohara T, Shintani S, Kondo K. Autologous adipose-derived regenerative cells for therapeutic angiogenesis. *Current pharmaceutical design* 2009; 15: 2784-2790.

90. Li W, Liu Y, Zhang P, et al. Tissue-Engineered Bone Immobilized with Human Adipose Stem Cells-Derived Exosomes Promotes Bone Regeneration.*ACS applied materials & interfaces* 2018; 10: 5240-5254.

91. Kuterbekov M, Jonas AM, Glinel K, et al. Osteogenic differentiation of adipose derived stromal cells: from bench to clinics. *Tissue engineering Part B, Reviews* 2020.

Posted on Authorea 31 Jul 2020 — CC0 1.0 — https://doi.org/10.22541/au.159620994.43378706 — This a preprint and has not been peer reviewed. Data may be preliminary.